Distributed Control for 3D Inspection using Multi-UAV Systems

Angelos Zacharia, Savvas Papaioannou, Panayiotis Kolios, and Christos Panayiotou

***Abstract*—Cooperative control of multi-UAV systems has attracted substantial research attention due to its significance in a variety of application sectors, such as emergency response, search-and-rescue missions, and critical infrastructure inspection. This paper proposes a distributed control algorithm for generating collision-free trajectories that drive the multi-UAV system to completely inspect a set of 3D points on the surface of an object of interest. The UAVs' objective is to cooperatively inspect the object of interest in the minimum amount of time. Extensive numerical simulations for a team of quadrotor UAVs inspecting a real 3D structure illustrate the validity and effectiveness of the proposed approach.**

***Index Terms*—Distributed control, 3D inspection, multi-UAV systems**

I. Introduction

Unmanned Aerial Vehicles (UAVs) have become increasingly popular in recent years due to their adaptability and wide range of uses. UAVs equipped with complementary sensor payloads such as cameras, radars, and navigation systems (e.g. GPS), allow their usage for various applications, such as surveillance [1], [2], emergency response missions [3], [4], security [5], [6], and inspection [7], [8]. The ability of UAVs to access hard-to-reach or dangerous regions is exploited to provide a cost-effective and efficient solution for several tasks.

One of the most prevalent applications of automated UAV-based systems is the inspection/coverage of an object of interest (e.g. collapsed buildings, critical infrastructures, sensitive facilities), which involves the process of determining the trajectory of a UAV to fully inspect/cover a specific area effectively. However, inspection/coverage planning for UAVs is a challenging problem due to balancing multiple objectives such as inspection quality and completeness, mission duration, and energy consumption. Inspection/coverage trajectory planning aims to ensure that each UAV agent provides detailed information about the object being inspected using technological equipment, such as gimballed camera and/or LiDAR while not violating the UAV's dynamics and sensing constraints as well as reducing the risk of collisions.

In the literature, several methodologies are proposed for solving the 3D inspection/coverage planning problem using UAVs, however, none of them handle all the aforementioned objectives and constraints. Consequently, in this work, the 3D inspection planning problem using a multi-UAV system is investigated for the complete inspection of an object of interest. In more detail, the object of interest comprises a finite number of distinct 3D points on its surface that are to be cooperatively inspected by multiple quadrotor UAVs. We assume that each UAV is identical to the other, that is, all UAVs are governed by the same dynamical model and have similar sensing capabilities. Accepting the above assumptions, we propose a 3D inspection planning algorithm for a team of UAVs, that determines the distributed control inputs of each UAV, ensuring that the resulting trajectories enable the complete inspection of the object of interest. The inspection trajectories are computed in an online fusion by each UAV using only local measurements and shared information from its neighbors. The contributions of the paper can be outlined as follows:

- We propose an online trajectory planning algorithm that enables the multi-UAV system to fully inspect large-scale complex structures in the 3D environment.
- We design a distributed control scheme for each UAV that only uses local measurements, e.g. UAV's position and velocity, and neighbors' position.

The rest of the paper is organized as follows. Section II presents an overview of the related work on inspection/coverage path and trajectory planning approaches. In Section III, we develop the system model based on our modeling assumptions, while the problem addressed by this work is outlined in Section IV. In the sequel, Section V discusses the details of the proposed 3D inspection approach, and Section VI evaluates the proposed methodology. Finally, Section VII concludes the paper and discusses future work.

II. Related Work

In recent years, a plethora of methodologies have been proposed for solving the well-established problem of inspection/coverage planning using single-robot or multi-robot systems. A comprehensive categorization of the various inspection/coverage planning strategies is presented by the survey [9], [10]. This section briefly discusses the most significant approaches that find a solution for the 2D or 3D inspection/coverage planning problem. The proposed techniques in the literature are separated into Coverage Path Planning (CPP) and Coverage Trajectory Planning (CTP) approaches. The main difference between these two techniques is that CPP reformulates the aforementioned problem into a more straightforward path planning problem, neglecting the robot's dynamics, and only generates paths that the inspection of the area of interest (AOI) is guaranteed. On the other hand,

The authors are with the KIOS Research and Innovation Center of Excellence (KIOS CoE) and the Department of Electrical and Computer Engineering, University of Cyprus, Nicosia, 1678, Cyprus.{zacharia.angelos, papaioannou.savvas, pkolios, christosp}@ucy.ac.cy

CTP finds the robot's control input that generates a trajectory capable of inspecting the AOI.

Initially, the problem of 2D inspection/coverage planning was primarily conducted with single-robot systems. In particular, a boustrophedon cellular decomposition of the 2D collision-free space is proposed in [11], creating a number of non-intersecting cells. Then, a path-finding problem is solved by providing the robot's path that covers all cells with back-and-forth motions. The authors in [12] develop an algorithm for inspecting the object's boundary in a planar environment. The complete inspection of the object's boundary is achieved by selecting and connecting constraint sensing positions. The work in [13] addresses the coverage of non-overlapping cells with sweeping motions whereas the authors in [14], investigate optimal sweeping direction to generate the decomposition of the environment. Instead of the static decomposition of the area, the authors in [15], propose an incremental construction of cell decomposition at the same time as the robot covers the area of interest.

Furthermore, the use of multi-robot systems appears in the literature for solving the 2D inspection/coverage planning problem. In [16], three different multi-robot coverage approaches are presented where all utilize the boustrophedon cellular decomposition, while a method for planning the multi-UAV coverage paths in a polygon region of interest is proposed in [17] based on an exact cellular decomposition. For a team of small UAVs, [18] presents a cell decomposition algorithm that uses regular hexagons for area coverage, and in [19], a time-based optimal solution is proposed by reformulating the multi-robot coverage path planning into single-robot problems. The vast majority of the previously stated 2D inspection/coverage planning algorithms cannot be expanded to the 3D inspection/coverage planning problem.

By switching to the more complex 3D environment, the problem of 3D inspection/coverage planning becomes more challenging. The authors in [20] extract stationary viewpoints for an underwater inspection robot that ensures complete coverage based on both the redundant roadmap and watchman route algorithms. A traveling salesman problem (TSP) is then solved to find a feasible path for ship hull inspection. Similarly, in [21], a sampling-based view planning approach using a UAV is proposed. The 3D inspection/coverage planning is transformed to a mixed integer quadratic programming in [22], [23], generating UAV trajectories capable to cover cuboid-like objects of interest. Our previous work in [24] proposes a UAV-based receding horizon inspection planning control methodology that generates an optimal trajectory for inspecting crucial feature-points on the object's surface. For a 3D surface inspection, the authors in [25] propose an online approach that consists of the optimal control waypoints extraction process and the generation of the UAV's continuous trajectory from these points. The work in [26] presents a path primitive sampling technique to plan the UAV's path for visual inspection of the structure of interest. In summary, the aforementioned studies provide a solution to the 3D inspection/coverage problem using a single-robot system. However, these methodologies are improper for handling the multi-robot 3D inspection/coverage planning problem due to their system setup. On the contrary, the work in [27] proposes a cluster-based next-best-view planning method for online surface reconstruction of complex environments using multiple UAVs. Furthermore, the authors in [28] solve the problem of coverage path planning using multiple UAVs for the inspection of large-scale 3D structures. The aforementioned problem is reformulated to a set-covering vehicle routing problem, which is solved by a modified biased random key genetic algorithm. The works [27], [28] reformulate the problem of the multi-robot 3D inspection/coverage planning into a more straightforward CPP, neglecting the robot's dynamics, and only generating paths that guarantee the inspection of the area of interest.

A few recent related works also investigate the multi-UAV 3D inspection/coverage trajectory planning problem. For instance, the work in [29] examines the cooperative inspection problem of a complex 3D structure using a UAV team. Complete coverage is accomplished by the infrastructure's surface division and the assignment of the resulting areas to each UAV. Then the problem is formulated as a multi travelling salesman problem. In [30] the authors proposed a trajectory planner for a team of multiple UAVs, based on the particle swarm optimization approach which finds the optimal trajectories utilizing distributed full coverage and a dynamic fitness function. Finally, the authors in [31] propose a heat equation driven area coverage methodology for visual inspection of 3D complex structures using a multi-UAV system. The algorithm produces collision-free trajectories and UAVs' camera orientations.

The primary limitation of the works mentioned above is the number of robots used to solve that problem. An offline optimization of the single-robot path does not reduce the inspection time dramatically compared with the use of a multi-robot system, which provides faster and more robust 3D inspection. Centralized or decentralized planners are utilized to generate the robots' trajectories, however, in our proposed method the 3D inspection trajectory is planned in a distributed manner, that enables the implementation using only local measurements and information exchanged only between neighboring agents.

III. System Model

A. UAV Dynamics

A quadrotor UAV maneuvers inside a bounded and convex region $\mathcal{Q} \subset \mathbb{R}^3$. Let $\mathbf{E} = \{x_\mathbf{E}, y_\mathbf{E}, z_\mathbf{E}\}$ be the earth-fixed coordinate frame, which is placed arbitrary in 3D space. On a quadrotor UAV is attached a body-fixed coordinate frame $\mathbf{B} = \{x_\mathbf{B}, y_\mathbf{B}, z_\mathbf{B}\}$, whose origin coincides with the center of mass of the agent. The nonlinear dynamical model of a quadrotor UAV, based on [32], can be expressed as:

$$\dot{\mathbf{p}} = \boldsymbol{v} \tag{1}$$

$$\dot{\boldsymbol{v}} = -g\mathbf{e}_3^\mathbf{E} + \frac{1}{m}\mathbf{R}F\mathbf{e}_3^\mathbf{B} \tag{2}$$

$$\mathbf{I}\dot{\boldsymbol{\Omega}} = -\boldsymbol{\Omega} \times \mathbf{I}\boldsymbol{\Omega} + \boldsymbol{\tau} \tag{3}$$

where the UAV's position is denoted by $\mathbf{p} = [x, y, z]^T \in \mathbf{E}$, $\boldsymbol{v} \in \mathbf{E}$ is the linear velocity vector, $\boldsymbol{\Omega} \in \mathbf{B}$ represents the angular velocity, $\mathbf{I} \in \mathbb{R}^{3\times3}$ describes the inertia matrix, and $\boldsymbol{\tau}$ is the total torque applied to the UAV. Furthermore, g is the gravitational acceleration, m is the UAV's mass, $\mathbf{e}_3^{\mathbf{E}} = \mathbf{e}_3^{\mathbf{B}} = [0, 0, 1]^T$, the thrust input to the UAV is denoted by F, and the rotation matrix $R \in SO(3)$ is defined as:

$$\mathbf{R} = \begin{bmatrix} c_\psi c_\theta & -c_\theta s_\psi & s_\theta \\ c_\phi s_\psi + c_\psi s_\phi s_\theta & c_\phi c_\psi - s_\phi s_\psi s_\theta & -c_\theta s_\phi \\ s_\phi s_\psi - c_\phi c_\psi s_\theta & c_\psi s_\phi + c_\phi s_\psi s_\theta & c_\phi c_\theta \end{bmatrix}, \quad (4)$$

where $c_\alpha = \cos\alpha$, $s_\alpha = \sin\alpha$, and ϕ, θ, and ψ are the roll, pitch, and yaw Euler's angles, respectively.

The complex UAV dynamics can be simplified by adopting the feedback linearization control technique, which enables the use of linear controllers. In general, the UAV dynamics can be hierarchically controlled by two steps, i.e. the position and attitude control, assuming however, that the attitude dynamics converges faster than the translational dynamics [33], [34]. Thus, in this work, we design a control scheme only for translational dynamics (1)-(2). Introducing auxiliary control inputs, we define the total thrust F, and the desired roll ϕ_d and pitch θ_d as follows

$$\begin{aligned} F &= \frac{m(u_z + g)}{c_\theta c_\phi}, \\ \phi_d = \arctan\left(-\frac{u_y}{u_z + g}\right), &\quad \theta_d = \arctan\left(\frac{u_x c_\phi}{u_z + g}\right). \end{aligned} \quad (5)$$

Note that the selection of the rotational matrix $\mathbf{R}$ imposes the yaw angle ψ to be zero, and therefore it is absent from the translational dynamics. By substituting (5) in (2), we obtain the reduced translational dynamics as:

$$\begin{aligned} \dot{\mathbf{p}} &= \boldsymbol{v} \\ \dot{\boldsymbol{v}} &= \boldsymbol{u} \end{aligned} \quad (6)$$

where $\boldsymbol{u} = [u_x, u_y, u_z]^T \in \mathbb{R}^{3\times1}$ is the auxiliary control input vector.

B. Object 3D Representation

The 3D representation of an object of interest $\mathcal{W} \subset \mathcal{Q}$ requires numerous calibrated images to be gathered during the 3D reconstruction process [35]. A 3D point-cloud $\mathcal{Q}_c = \{q_c^l\}$, $l \in \{1, \ldots, |\mathcal{Q}_c|\}$, is extracted from these images, with points $q_c \in \mathcal{Q}_c$ being part of the surface area on the object's boundary $\partial\mathcal{W}$. Utilizing the Delaunay triangulation method [36], a triangle mesh $\mathcal{K}$ is constructed consisting of triangular facets $\kappa \in \mathcal{K}$, as depicted in Figure 1. Furthermore, the center of each triangular facet $q_\kappa \in \mathcal{Q}_\kappa$ is generated and combined with the 3D point-cloud set $\mathcal{Q}_c$, forming the target set $\mathcal{Q}_T = \{\mathcal{Q}_c \cup \mathcal{Q}_\kappa\}$.

IV. Problem Statement

Consider a group of N quadrotor UAVs, with dynamics described by (6), being located at an arbitrary area inside the bounded and convex inspection region $\mathcal{Q} \subset \mathbb{R}^3$. It is assumed

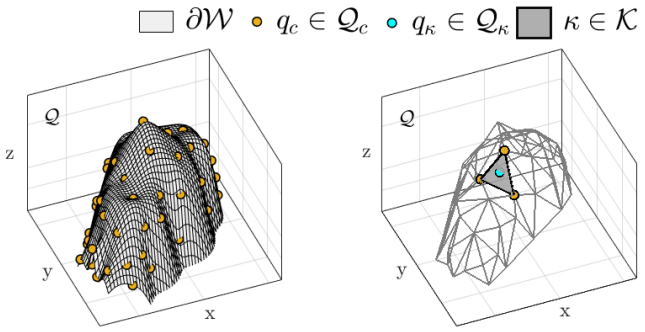

Fig. 1: A 3D point-cloud $\mathcal{Q}_c$ generation from the object's boundary $\partial\mathcal{W}$ and its Delaunay triangulation, forming a triangular mesh $\mathcal{K}$.

that each UAV $i \in \mathcal{V}$, where $\mathcal{V} = \{1, \ldots, N\}$, is equipped with a gimballed camera that has the capability to rotate its field-of-view (FoV) to any direction in $\mathcal{Q}$, capturing important information of the environment. Let an object of interest, e.g. a structure, be represented by a surface from which a set of points $\mathcal{Q}_T = \{\mathbf{q}_T^l\}$, $l \in \{1, \ldots, |\mathcal{Q}_T|\}$ is extracted, where $\mathbf{q}_T^l$ is the k^{th} target point on the object's boundary $\partial\mathcal{W}$, and the total number of these points is denoted by $|\mathcal{Q}_T|$. The target points that need to be inspected are already known to the UAVs. The 3D inspection problem addressed in this work can be stated as follows: *Find for each quadrotor UAV $i \in \mathcal{V}$ a distributed control law, such that, for any initial positions $\mathbf{p}_i(0)$ of each UAV $i \in \mathcal{V}$, the multi-UAV system cooperatively inspects all target points $\mathcal{Q}_T$ on the object's boundary $\partial\mathcal{W}$, and all signals remain bounded.* The aforementioned problem can be expressed at a high level, as formed in Problem (P1).

Problem (P1): *3D Inspection Problem*

$$\underset{\boldsymbol{u}_1(t), \ldots, \boldsymbol{u}_N(t)}{\operatorname{argmin}} \quad \mathcal{H}, \quad t \geq 0 \quad (7a)$$

subject to:

$$\dot{\mathbf{p}}_i(t) = \boldsymbol{v}_i(t), \quad \dot{\boldsymbol{v}}_i(t) = \boldsymbol{u}_i(t) \qquad \forall i \in \mathcal{V}, \forall t \geq 0 \quad (7b)$$

$$\mathbf{p}_i(t) \in \mathcal{Q} - \mathcal{W} \qquad \forall i \in \mathcal{V}, \forall t \geq 0 \quad (7c)$$

$$\mathbf{p}_i(t) \neq \mathbf{p}_j(t) \qquad \forall i, j \in \mathcal{V}, \forall t \geq 0 \quad (7d)$$

The objective is to design, for each UAV $i \in \mathcal{V}$, a control input $\boldsymbol{u}_i(t)$ that the trajectories of the multi-UAV system drive the inspection cost function $\mathcal{H}$ to the minimizer, subject to the constraints in (7b)-(7d). The constraint in (7b) corresponds to the UAVs' dynamics introduced in (6) while the constraint (7c) ensures that the position of any UAV $i \in \mathcal{V}$ for $\forall\ t \geq 0$, belongs to the inspection region $\mathcal{Q}$ avoiding collision with the object of interest $\mathcal{W}$. Finally, the inter-agent collision avoidance is represented by the constraint in (7d).

V. Proposed Approach

A. Cost Function

Consider a multi-UAV system consisting of N quadrotor UAVs. Let $\mathcal{Q} \subset \mathbb{R}^3$ be a convex region in which the UAVs move and the position of the i^{th} UAV is denoted by $\mathbf{p}_i$. The set

of all UAVs' positions is also defined as $\mathcal{P} = \{\mathbf{p}_1, \ldots, \mathbf{p}_N\}$. The sensing quality at the point $\mathbf{q} \in \mathcal{Q}$ measured by the i^{th} UAV located at $\mathbf{p}_i$ decreases proportionally with the distance $\|\mathbf{q} - \mathbf{p}_i\|$. This measure can be expressed by an isotropic, strictly increasing, and convex function $f(\|\mathbf{q} - \mathbf{p}_i\|) : \mathbb{R}_+ \to \mathbb{R}_+$, called sensing unreliability function, that as reaches large values, the sensing quality deteriorates. The function $\varphi : \mathcal{Q} \to \mathbb{R}_+$ is a density function over $\mathcal{Q}$ that allocates weight to each point $\mathbf{q} \in \mathcal{Q}$ in the region, signifying the relative importance of various regions in $\mathcal{Q}$. As a result, the multi-UAV team focuses on areas with high values of $\varphi(\mathbf{q})$. Given the set $\mathcal{P}$, the optimal partition of $\mathcal{Q}$ can be obtained by constructing the set of Voronoi regions, $V = \{V_1, V_2, ..., V_N\}$, where the UAVs positions are the generating points, as:

$$V_i = \{\mathbf{q} \in \mathcal{Q} : \|\mathbf{q} - \mathbf{p}_i\| \leq \|\mathbf{q} - \mathbf{p}_j\|, \ \forall\ j \neq i\}. \quad (8)$$

If the Voronoi regions V_i and V_j are adjacent, that is, it holds true that $V_i \cap V_j \neq 0$, then the i^{th} and j^{th} are called neighbors. The neighborhood of the i^{th} UAV is denoted by $\mathcal{N}_i$ comprising all the UAV neighbors.

The inspection cost function is thereafter defined as an indicator of multi-UAV system performance as follows:

$$\mathcal{H}(\mathcal{P}) = \sum_{i=1}^{N} \int_{V_i} f(\|\mathbf{q} - \mathbf{p}_i\|)\varphi(\mathbf{q}) d\mathbf{q}. \quad (9)$$

The function $\mathcal{H}$ measures how ineffectively the UAVs are positioned inside $\mathcal{Q}$ based on its importance regions, and therefore the multi-UAV system aims to minimize it. One way to find the minimizer of $\mathcal{H}$ is to compute its gradient concerning the UAVs' positions $\mathbf{p}_i$, which is given by, [37]:

$$\frac{\partial \mathcal{H}}{\partial \mathbf{p}_i} = \int_{V_i} \frac{\partial f(\|\mathbf{q} - \mathbf{p}_i\|)}{\partial \mathbf{p}_i} \varphi(\mathbf{q}) d\mathbf{q} = M_{V_i}(\mathbf{p}_i - \mathbf{C}_{V_i}) \quad (10)$$

where we utilize the quadratic sensing unreliability function as $f(\|\mathbf{q} - \mathbf{p}_i)\|) = \frac{1}{2}\|\mathbf{q} - \mathbf{p}_i\|^2$, and the mass M_{V_i} and centroid $\mathbf{C}_{V_i}$ of the Voronoi region V_i are respectively expressed as:

$$M_{V_i} = \int_{V_i} \varphi(\mathbf{q}) d\mathbf{q}, \quad \mathbf{C}_{V_i} = \frac{1}{M_{V_i}} \int_{V_i} \mathbf{q}\varphi(\mathbf{q}) d\mathbf{q}. \quad (11)$$

It is obvious that the partial derivative with respect to the i^{th} UAV position is determined only by its own position and the positions of its Voronoi neighbors. The equilibrium points of $\mathcal{H}$ can be found when $\partial\mathcal{H}/\partial\mathbf{p}_i = 0$, that is, $\mathbf{p}_i = \mathbf{C}_{V_i}$ for all $i \in \mathcal{V}$. Therefore, the multi-UAV system achieves Centroidal Voronoi Tessellation (CVT) by each UAV being positioned at the centroid of its Voronoi region.

B. 3D Target Points Inspection

As mentioned before, the goal of the multi-UAV system is to inspect a set of target points $\mathcal{Q}_T$ on the surface of the object's boundary $\partial\mathcal{W}$. We propose the outward projection of these points $\bar{\mathcal{Q}}_T = \{\bar{\mathbf{q}}_T^l\}$, $l \in \{1, \ldots, |\bar{\mathcal{Q}}_T|\}$, as shown in Figure 2, as a method of driving each UAV $i \in \mathcal{V}$ to positions around the projected points that are capable of inspecting the corresponding target points on the object's surface. More specifically, at each projected target point $\bar{\mathbf{q}}_T^l$, we attach a

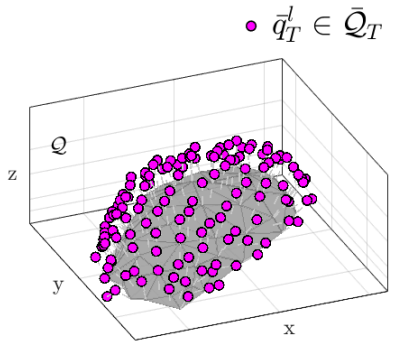

Fig. 2: 3D Projected Target points

3D Gaussian function $\varphi_l(\mathbf{q}, \bar{\mathbf{q}}_T^l)$ centered at $\bar{\mathbf{q}}_T^l$, and thus the density function $\varphi(\mathbf{q})$ can be defined as follows:

$$\varphi(\mathbf{q}) = \sum_{l=1}^{|\bar{\mathcal{Q}}_T|} b_l \varphi_l(\mathbf{q}, \bar{\mathbf{q}}_T^l) = \sum_{l=1}^{|\bar{\mathcal{Q}}_T|} b_l \alpha e^{-\beta\|\mathbf{q} - \bar{\mathbf{q}}_T^l\|^2}, \quad (12)$$

where $\alpha, \beta > 0$, $|\bar{\mathcal{Q}}_T|$ is the total number of the projected target points, and b_k is a binary variable that represents the target inspection status of $\mathbf{q}_T^l$. It is required that all target points are known to the UAVs and a set $\mathcal{B}_i = \{b_l\}$, $\forall\ l \in \{1, \ldots, |\mathcal{Q}_T|\}$ is stored by the UAV $i \in \mathcal{V}$ and shared to each neighbor $j \in \mathcal{N}_i$. A target point $\mathbf{q}_T^l$ is considered as inspected from the multi-UAV system if the following condition holds:

$$f(\|\bar{\mathbf{q}}_T^l - \mathbf{p}_i\|) = \frac{1}{2}\|\bar{\mathbf{q}}_T^l - \mathbf{p}_i\|^2 \leq r \quad i \in \mathcal{V}. \quad (13)$$

The inequality in Eqn. (13) can be interpreted as follows. If a UAV $i \in \mathcal{V}$ is positioned within a radius $r \in \mathbb{R}_+$ from the projected target point $\bar{\mathbf{q}}_T^l$, then it is assumed to acquire significant information about the target point $\mathbf{q}_T^l$, by rotating its camera's FoV to that direction. Therefore, the UAV $i \in \mathcal{V}$ has inspected $\mathbf{q}_T^l$, and sets $\mathcal{B}_{i,l} = b_l = 0$. The updated target inspection status set $\mathcal{B}_i$ is shared with the UAV's neighbors and the density function is computed again. This procedure is repeated until all target points are inspected from the multi-UAV system (see Algorithm 1).

C. Object Avoidance

During the mission of the multi-UAV system, each UAV $i \in \mathcal{V}$ moves towards the centroid $\mathbf{C}_{V_i}$ of its Voronoi region V_i. However, this movement generates a trajectory that may cause a collision between the UAV and the object of interest. Consequently, an object avoidance technique is adopted to maintain the UAVs' positions $\mathbf{p}_i \in \mathcal{Q} - \mathcal{W}$. As mentioned above, the object of interest is represented by a set of target points $\mathcal{Q}_T$ which all UAVs should avoid due to disastrous consequences. As a result, a repulsive function is utilized as:

$$U_{o,i} = \begin{cases} \sum_{k=1}^{|\mathcal{Q}_T|} \frac{1}{2}\epsilon \left(\frac{1}{\|\mathbf{p}_i - \mathbf{q}_T^l\|} - \frac{1}{d_o}\right)^2, & \text{if } \|\mathbf{p}_i - \mathbf{q}_T^l\| \leq d_o \\ 0, & \text{otherwise} \end{cases} \quad (14)$$

where $\epsilon, d_o > 0$ are a positive gain and the safety distance, that is, the minimum allowable distance of the UAV $i \in \mathcal{V}$ from each target point $\mathbf{q}_T^l$, respectively.

D. Distributed Control Design

In this section, a distributed inspection control law is designed for each UAV $i \in \mathcal{V}$, governed by (6), that drives the multi-UAV system to inspect an object of interest. The following standard assumptions are made for achieving this goal.

Assumption 1: Each quadrotor UAV is capable to compute its own Voronoi region in a distributed way.

Assumption 2: Each quadrotor UAV has the ability to communicate with its Voronoi neighbors and share information.

A distributed control law, based on the Centroidal Voronoi Configuration (CVC), $\boldsymbol{u}_{c,i}$ is developed such that each UAV $i \in \mathcal{V}$ moves to its centroid C_{V_i}. Therefore, the following position controller for the i^{th} UAV is given by:

$$\boldsymbol{u}_{c,i} = k_p M_{V_i} \mathbf{C}_{V_i} - (k_p M_{V_i} \mathbf{p}_i + k_d \boldsymbol{v}_i) \tag{15}$$

where $k_p, k_d > 0$ are the proportional and derivative control gains, respectively.

Proposition 1: Consider a group of N quadrotor UAVs, with dynamics governed according to (6). If Assumptions 1 and 2 hold, and the control scheme (15) is employed for each UAV $i \in \mathcal{V}$, then it is guaranteed that the multi-UAV system is asymptotically stable, and the UAVs move towards the CVC until the object of interest is totally inspected.

Proof. We define a candidate Lyapunov function as

$$\Upsilon = k_p \mathcal{H} + \sum_{i=1}^{N} \frac{1}{2} \boldsymbol{v}_i^T \boldsymbol{v}_i \tag{16}$$

Taking the time derivative of Υ along the system trajectories, and using (6), (10),(15), we obtain that

$$\begin{aligned}
\dot{\Upsilon} &= \sum_{i=1}^{N} k_p \frac{\partial \mathcal{H}}{\partial \mathbf{p}_i}^T \dot{\mathbf{p}}_i + \sum_{i=1}^{N} \boldsymbol{v}_i^T \dot{\boldsymbol{v}}_i \\
&= \sum_{i=1}^{N} \boldsymbol{v}_i^T \big(k_p M_{V_i} (\mathbf{p}_i - \mathbf{C}_{V_i}) + k_p M_{V_i} \mathbf{C}_{V_i} \\
&\qquad - (k_p M_{V_i} \mathbf{p}_i + k_d \boldsymbol{v}_i) \big) \\
&= \sum_{i=1}^{N} -k_d \boldsymbol{v}_i^T \boldsymbol{v}_i,
\end{aligned} \tag{17}$$

which is negative semidefinite, that is, the asymptotic stability of the system cannot be proven. However, suppose that S is the set of all trajectories that keep $\dot{\Upsilon} \leq 0$. Since the trajectories of the closed-loop system are inside the convex region $\mathcal{Q}$, S is a positive invariant set. Invoking the LaSalle invariance principle, we can conclude about the stability of the system as follows:

$$\dot{\Upsilon} = 0 \implies \boldsymbol{v}_i = 0 \implies \dot{\boldsymbol{v}}_i = 0 \implies \boldsymbol{u}_i = 0 \implies \mathbf{p}_i = C_{V_i}$$

Therefore, for each UAV, $\mathbf{p}_i = C_{V_i}$ is the largest invariant set corresponding to the CVC. As a result, the closed-loop system is asymptotically stable. □

Remark 1: The computation of the control scheme (15) requires the i^{th} UAV to communicate with its Voronoi neighbors in order to compute the mass and centroid of its Voronoi region. As a result, this control scheme is considered distributed.

Remark 2: The i^{th} UAV's motion tends to the centroid of its Voronoi region when the control scheme (15) is employed. Since the centroid always lies inside the Voronoi region, and the Voronoi tessellations generate non-overlapping regions, there will be no inter-UAV collision during the mission.

By applying the proposed control law (15), object avoidance is not guaranteed, as it does not involve any movement restriction of the UAV $i \in \mathcal{V}$. Due to this fact, it is essential to combine the PD control law $\boldsymbol{u}_{c,i}$ with an obstacle avoidance control law $\boldsymbol{u}_{o,i} = -\nabla_{\mathbf{p}_i} U_{o,i}$ such that the augmented control scheme forces the multi-UAV system to reach its goal safely. We proposed the following control scheme

$$\boldsymbol{u}_i = \boldsymbol{u}_{c,i} + \boldsymbol{u}_{o,i} \tag{18}$$

with

$$\boldsymbol{u}_{o,i} = \sum_{l=1}^{|\mathcal{Q}_T|} \mu_o c_{il} \left(\frac{1}{\|\mathbf{p}_i - \mathbf{q}_T^l\|} - \frac{1}{d_o} \right) \frac{\mathbf{p}_i - \mathbf{q}_T^l}{\|\mathbf{p}_i - \mathbf{q}_T^l\|^2} \tag{19}$$

where μ_o is the gain of the obstacle-free term, d_o is the minimum-accepted distance between UAV i and the object's boundary, and the binary variable c_{il}, $\forall\ i \in \mathcal{V}$ and $\forall\ l \in \{1, \ldots, |\mathcal{Q}_T|\}$ is defined as:

$$c_{il} = \begin{cases} 1, & \forall\ \|\mathbf{p}_i - \mathbf{q}_T^l\| \leq d_o \\ 0, & \text{otherwise.} \end{cases} \tag{20}$$

The stability of the multi-UAV system utilizing the augmented control scheme (18), can be proved by considering the following two cases. In the case that the UAV $i \in \mathcal{V}$, is outside any repulsive region, that is, $\|\mathbf{p}_i - \mathbf{q}_T^l\| \geq d_o$, $\forall\ l \in \{1, \ldots, |\mathcal{Q}_T|\}$, all binary variables $c_{il} = 0$ which remove the obstacle avoidance term from the proposed control law. Consequently, (17) holds true and the system is asymptotically stable, as proved previously. Now, consider that the UAV $i \in \mathcal{V}$ is inside at least one repulsive region such that $\|\mathbf{p}_i - \mathbf{q}_T^l\| < d_o$, thus the corresponding binary variables $c_{il} = 1$, and $\boldsymbol{u}_{o,i} \neq 0$. Modifying the candidate Lyapunov function Υ to be $\Upsilon = k_p \mathcal{H} + \sum_{i=1}^{N} \frac{1}{2} \boldsymbol{v}_i^T \boldsymbol{v}_i + \sum_{i=1}^{N} U_{c,i}$, and employed the control law $\boldsymbol{u}_i$, as in (18), then it is proved again the asymptotic stability of the system.

As we have presented the entire methodology, the overall process is outlined in Algorithm 1. To summarize, each UAV obtains the position of its neighbors to calculate the centroid of its Voronoi region, which is utilized in the distributed control law. In addition, each UAV merges its target inspection status set with its corresponding neighbor sets, resulting in the updated density function that drives the UAV to uninspected regions.

Algorithm 1 3D Inspection Algorithm

Require: A group of UAVs $\mathcal{V} = \{1, \ldots, N\}$, with initial positions $\mathbf{p}_i(0)$, $i \in \mathcal{V}$, are located inside the inspection region $\mathcal{Q} \in \mathbb{R}^3$. Target points $\mathbf{q}_T^l \in \mathcal{Q}_T$ are known to the multi-UAV system. Each UAV $i \in \mathcal{V}$ should be able to compute its Voronoi region V_i, and share information with its Voronoi neighbors.

Ensure: Complete inspection of the target points $\mathbf{q}_T^l \in \mathcal{Q}_T$.

while $\mathcal{B}_i \neq \emptyset$ **do**
  Acquires the position $\mathbf{p}_j$ and target inspection status set $\mathcal{B}_j$, $\forall\ j \in \mathcal{N}_i$
  Updates the set $\mathcal{B}_i = \mathcal{B}_i \vee \mathcal{B}_j$
  Constructs its Voronoi region $V_i(\mathbf{p}_i, \mathbf{p}_j)$, as in (8)
  Computes the centroid $\mathbf{C}_{V_i}$ of its $V_i(\mathbf{p}_i, \mathbf{p}_j)$, as in (11)
  Computes and applies the control input $\boldsymbol{u}_i$, as in (18)
  Update the target inspection status $\mathcal{B}_i$:
  if $f(\|\bar{\mathbf{q}}_T^l - \mathbf{p}_i\|) \leq r$ **then**
    $\mathcal{B}_{i,k} = 0$, $\forall\ l \in \{1, \ldots, |\mathcal{Q}_T|\}$
  end if
end while

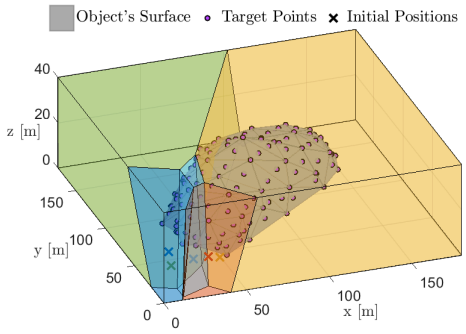

Fig. 3: Voronoi tessellation of the inspection region at $t = 0$.

VI. Evaluation

Numerous simulations have been performed to demonstrate the efficacy of the proposed methodology for the 3D inspection of an object of interest by a multi-UAV system.

A. Simulation Setup

A numerical simulation is provided which was carried out in a MATLAB environment on a 2.8GHz desktop computer with 16GB of RAM. Consider a team of 5 quadrotor UAVs, with dynamics (6), which are initially located inside a cuboid inspection region of dimensions 180m $\times$ 180m $\times$ 40m. The objective of the multi-UAV system is to inspect an object of interest of dimensions 156m $\times$ 78m $\times$ 26m. More specifically, a set of 132 target points, being part of the object's surface and denoted by purple circles, have to be inspected by the multi-UAV system, as illustrated in Fig. 3. For achieving this goal, density functions are utilized with the parameters $\alpha = 1$ and $\beta = 0.0075$ while the sensing range of each UAV is chosen as $r = 10$m. The control gains are selected as $k_p = 0.32$, $k_d = 0.86$, and $\mu_o = 1000$ for a safety-region $d_o = 12$m.

B. Results

A group of five UAVs is initially located inside the inspection region at the random positions $\mathbf{p}_1^0 = [10, 20, 15]^T$m, $\mathbf{p}_2^0 = [30, 9, 14]^T$m, $\mathbf{p}_3^0 = [40, 17, 10]^T$m, $\mathbf{p}_4^0 = [15, 30, 5]^T$m, and $\mathbf{p}_5^0 = [25, 20, 10]^T$m, respectively. The initial Voronoi tessellation of the inspection region is constructed, as illustrated in Fig. 3, with the generating points being the initial positions of the UAVs. Each Voronoi cell is colored with the corresponding UAV's color.

In Fig. 4, we provide several simulation results. Initially, as mentioned in the methodology, we project the target points in order to generate collision-free trajectories that drive the multi-UAV system to inspect the object of interest, as shown in Fig. 4a. During the mission, when a UAV is located sufficiently close to a projected point, it automatically rotates its camera's FoV pointing to the corresponding target point on the object's surface, as depicted in Fig 4b. Thus, that point is captured from the camera's FoV with satisfactory quality. A facet consisting of four target points, the facet vertices and the face center, is considered inspected when all these target points lie in any UAV camera's FoV. Fig. 4c illustrates a time instant of the UAVs' trajectories and the inspected or uninspected facets. The UAV's trajectories that enable the full inspection of the object of interest are depicted in Fig. 4d. More precisely, a time-based facet inspection is provided in Fig. 4e which shows at which time a facet was inspected. Finally, the collision-free trajectories were generated utilizing the control inputs of Fig. 4f.

For further evaluation of the proposed methodology, the aforementioned setup is compared with two different case studies, using three UAVs and seven UAVs, respectively. As depicted in Fig. 5, the evolution of cost functions of all three case studies are compared. It is obvious that the setup with three UAVs needs the largest amount of time, $t_f^3 = 111.8$ s, in order to minimize its cost function compared with the other cases that need $t_f^5 = 38.6$ s, $t_f^7 = 32.8$ s respectively. As the number of UAVs is increasing, it is shown that the mission time for object inspection is decreasing. Fig. 6 illustrates the percentage of inspection completeness for the case studies. Up to $t = 10$ s, it is observed that the percentage of inspection completeness, for all the cases, is approximately the same. After that time, the inspection rates of both setups with five and seven UAVs are similar, while the inspection rate of the setup with three UAVs is slowed down. Furthermore, in all case studies the percentage of inspection completeness reaches 100 % which enables the full inspection of the object of interest.

VII. Conclusion

In this work, we have proposed a methodology that solves the problem of 3D object inspection using a multi-UAV system. The objective function was minimized by designing a distributed control law that generates safe trajectories for the multi-UAV system, achieving the complete object inspection. Finally, the effectiveness of the proposed approach was demonstrated through simulations. Future work may consider trajectory optimization and real-world experiments.

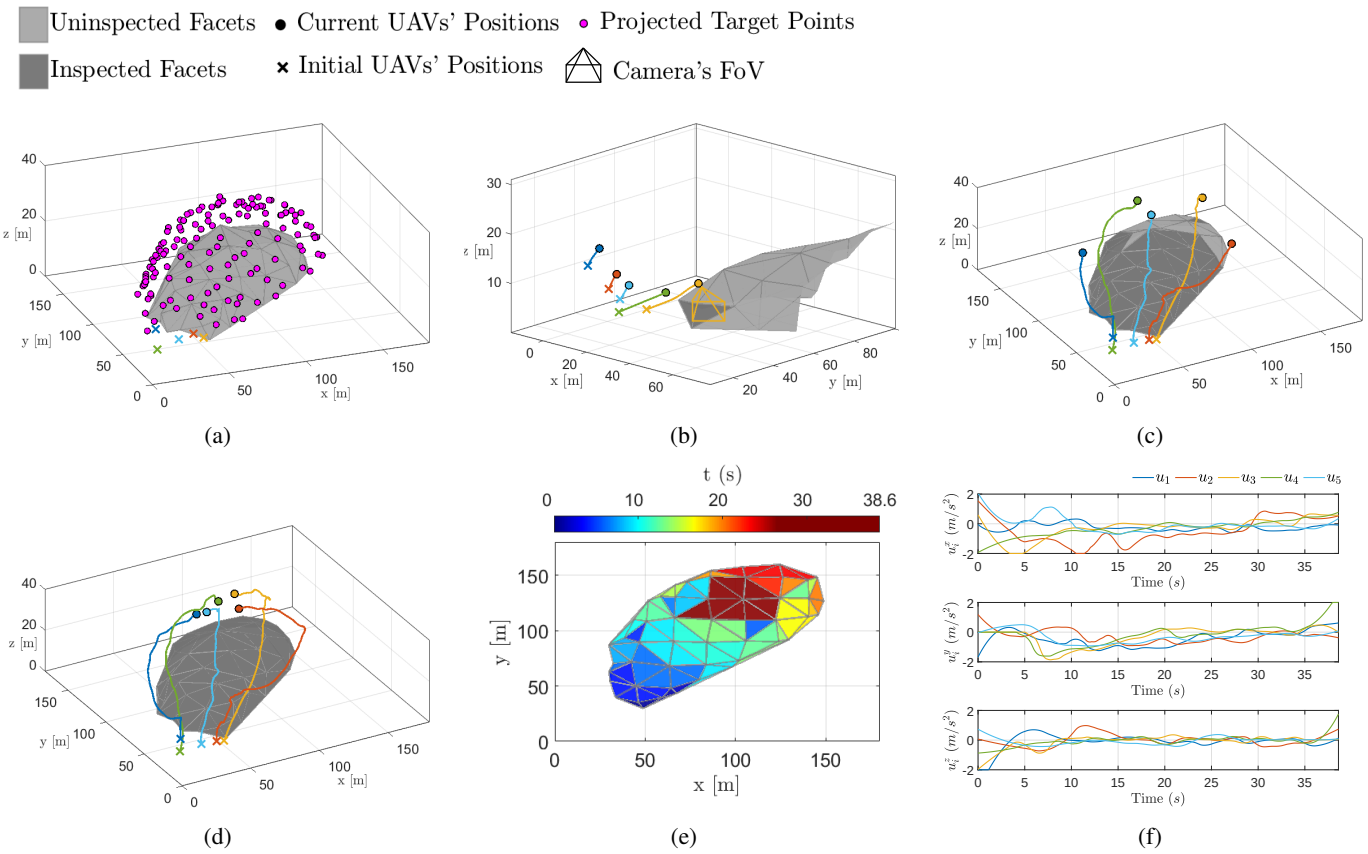

Fig. 4: Generated collision-free trajectories of a group of five UAVs for 3D inspection of the object of interest.

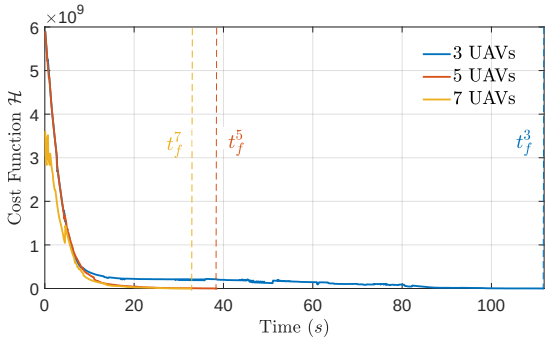

Fig. 5: Comparison of the inspection cost function $\mathcal{H}$ for three case studies.

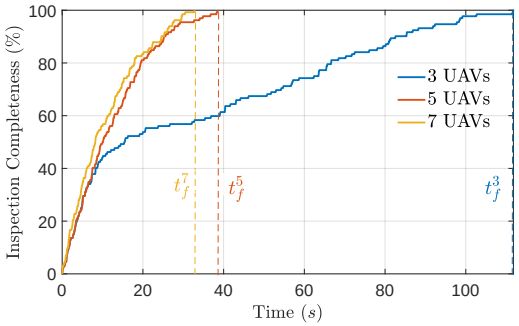

Fig. 6: Comparison of percentage inspection completeness for three case studies.

ACKNOWLEDGMENT

This work was undertaken as part of the GLIMPSE project EXCELLENCE/0421/0586 which is co-financed by the European Regional Development Fund and the Republic of Cyprus through the Research and Innovation Foundation's RESTART 2016-2020 Programme for Research, Technological Development and Innovation and supported by the European Union's Horizon 2020 research and innovation programme under grant agreement No 739551 (KIOS CoE), and from the Government of the Republic of Cyprus through the Cyprus Deputy Ministry of Research, Innovation and Digital Policy.

REFERENCES

[1] D. Kingston, S. Rasmussen, and L. Humphrey, "Automated uav tasks for search and surveillance," in *2016 IEEE Conference on Control Applications (CCA)*, pp. 1–8, IEEE, 2016.

[2] L. Geng, Y. Zhang, P. Wang, J. J. Wang, J. Y. Fuh, and S. Teo, "Uav surveillance mission planning with gimbaled sensors," in *11th IEEE international conference on control & automation (ICCA)*, pp. 320–325, IEEE, 2014.

[3] W. Jin, J. Yang, Y. Fang, and W. Feng, "Research on application and deployment of uav in emergency response," in *2020 IEEE 10th International Conference on Electronics Information and Emergency Communication (ICEIEC)*, pp. 277–280, IEEE, 2020.

[4] S. Papaioannou, P. Kolios, T. Theocharides, C. G. Panayiotou, and M. M. Polycarpou, "A cooperative multiagent probabilistic framework for search and track missions," *IEEE Transactions on Control of Network Systems*, vol. 8, no. 2, pp. 847–858, 2020.

[5] S. Papaioannou, P. Kolios, C. G. Panayiotou, and M. M. Polycarpou, "Cooperative simultaneous tracking and jamming for disabling a rogue drone," in *2020 IEEE/RSJ International Conference on Intelligent Robots and Systems (IROS)*, pp. 7919–7926, IEEE, 2020.

[6] N. Souli, R. Makrigiorgis, A. Anastasiou, A. Zacharia, P. Petrides, A. Lazanas, P. Valianti, P. Kolios, and G. Ellinas, "Horizonblock: implementation of an autonomous counter-drone system," in *2020 International Conference on Unmanned Aircraft Systems (ICUAS)*, pp. 398–404, IEEE, 2020.

[7] A. Savva, A. Zacharia, R. Makrigiorgis, A. Anastasiou, C. Kyrkou, P. Kolios, C. Panayiotou, and T. Theocharides, "Icarus: automatic autonomous power infrastructure inspection with uavs," in *2021 International Conference on Unmanned Aircraft Systems (ICUAS)*, pp. 918–926, IEEE, 2021.

[8] P. Ramon-Soria, M. Perez-Jimenez, B. Arrue, and A. Ollero, "Planning system for integrated autonomous infrastructure inspection using uavs," in *2019 International Conference on Unmanned Aircraft Systems (ICUAS)*, pp. 313–320, IEEE, 2019.

[9] E. Galceran and M. Carreras, "A survey on coverage path planning for robotics," *Robotics and Autonomous systems*, vol. 61, no. 12, pp. 1258–1276, 2013.

[10] C. S. Tan, R. Mohd-Mokhtar, and M. R. Arshad, "A comprehensive review of coverage path planning in robotics using classical and heuristic algorithms," *IEEE Access*, vol. 9, pp. 119310–119342, 2021.

[11] H. Choset and P. Pignon, "Coverage path planning: The boustrophedon cellular decomposition," in *Field and service robotics*, pp. 203–209, Springer, 1998.

[12] T. Danner and L. E. Kavraki, "Randomized planning for short inspection paths," in *Proceedings 2000 ICRA. Millennium Conference. IEEE International Conference on Robotics and Automation. Symposia Proceedings (Cat. No. 00CH37065)*, vol. 2, pp. 971–976, IEEE, 2000.

[13] Y. Gabriely and E. Rimon, "Spanning-tree based coverage of continuous areas by a mobile robot," *Annals of mathematics and artificial intelligence*, vol. 31, pp. 77–98, 2001.

[14] W. H. Huang, "Optimal line-sweep-based decompositions for coverage algorithms," in *Proceedings 2001 ICRA. IEEE International Conference on Robotics and Automation (Cat. No. 01CH37164)*, vol. 1, pp. 27–32, IEEE, 2001.

[15] E. U. Acar and H. Choset, "Sensor-based coverage of unknown environments: Incremental construction of morse decompositions," *The International Journal of Robotics Research*, vol. 21, no. 4, pp. 345–366, 2002.

[16] I. Rekleitis, A. P. New, E. S. Rankin, and H. Choset, "Efficient boustrophedon multi-robot coverage: an algorithmic approach," *Annals of Mathematics and Artificial Intelligence*, vol. 52, pp. 109–142, 2008.

[17] Y. Li, H. Chen, M. J. Er, and X. Wang, "Coverage path planning for uavs based on enhanced exact cellular decomposition method," *Mechatronics*, vol. 21, no. 5, pp. 876–885, 2011.

[18] H. I. Perez-Imaz, P. A. Rezeck, D. G. Macharet, and M. F. Campos, "Multi-robot 3d coverage path planning for first responders teams," in *2016 IEEE International Conference on Automation Science and Engineering (CASE)*, pp. 1374–1379, IEEE, 2016.

[19] A. C. Kapoutsis, S. A. Chatzichristofis, and E. B. Kosmatopoulos, "Darp: divide areas algorithm for optimal multi-robot coverage path planning," *Journal of Intelligent & Robotic Systems*, vol. 86, pp. 663–680, 2017.

[20] B. Englot and F. S. Hover, "Three-dimensional coverage planning for an underwater inspection robot," *The International Journal of Robotics Research*, vol. 32, no. 9-10, pp. 1048–1073, 2013.

[21] W. Jing, J. Polden, W. Lin, and K. Shimada, "Sampling-based view planning for 3d visual coverage task with unmanned aerial vehicle," in *2016 IEEE/RSJ International Conference on Intelligent Robots and Systems (IROS)*, pp. 1808–1815, IEEE, 2016.

[22] S. Papaioannou, P. Kolios, T. Theocharides, C. G. Panayiotou, and M. M. Polycarpou, "Towards automated 3d search planning for emergency response missions," *Journal of Intelligent & Robotic Systems*, vol. 103, no. 1, p. 2, 2021.

[23] S. Papaioannou, P. Kolios, T. Theocharides, C. G. Panayiotou, and M. M. Polycarpou, "3d trajectory planning for uav-based search missions: An integrated assessment and search planning approach," in *2021 International Conference on Unmanned Aircraft Systems (ICUAS)*, pp. 517–526, IEEE, 2021.

[24] S. Papaioannou, P. Kolios, T. Theocharides, C. G. Panayiotou, and M. M. Polycarpou, "Uav-based receding horizon control for 3d inspection planning," in *2022 International Conference on Unmanned Aircraft Systems (ICUAS)*, pp. 1121–1130, IEEE, 2022.

[25] H. Zhu, J. J. Chung, N. R. Lawrance, R. Siegwart, and J. Alonso-Mora, "Online informative path planning for active information gathering of a 3d surface," in *2021 IEEE International Conference on Robotics and Automation (ICRA)*, pp. 1488–1494, IEEE, 2021.

[26] W. Jing, D. Deng, Z. Xiao, Y. Liu, and K. Shimada, "Coverage path planning using path primitive sampling and primitive coverage graph for visual inspection," in *2019 IEEE/RSJ International Conference on Intelligent Robots and Systems (IROS)*, pp. 1472–1479, IEEE, 2019.

[27] G. Hardouin, J. Moras, F. Morbidi, J. Marzat, and E. M. Mouaddib, "Next-best-view planning for surface reconstruction of large-scale 3d environments with multiple uavs," in *2020 IEEE/RSJ International Conference on Intelligent Robots and Systems (IROS)*, pp. 1567–1574, IEEE, 2020.

[28] W. Jing, D. Deng, Y. Wu, and K. Shimada, "Multi-uav coverage path planning for the inspection of large and complex structures," in *2020 IEEE/RSJ International Conference on Intelligent Robots and Systems (IROS)*, pp. 1480–1486, IEEE, 2020.

[29] S. S. Mansouri, C. Kanellakis, E. Fresk, D. Kominiak, and G. Nikolakopoulos, "Cooperative coverage path planning for visual inspection," *Control Engineering Practice*, vol. 74, pp. 118–131, 2018.

[30] N. Ahmed, C. J. Pawase, and K. Chang, "Distributed 3-d path planning for multi-uavs with full area surveillance based on particle swarm optimization," *Applied Sciences*, vol. 11, no. 8, p. 3417, 2021.

[31] S. Ivić, B. Crnković, L. Grbčić, and L. Matleković, "Multi-uav trajectory planning for 3d visual inspection of complex structures," *Automation in Construction*, vol. 147, p. 104709, 2023.

[32] L. R. García Carrillo, A. E. Dzul López, R. Lozano, and C. Pégard, "Modeling the quad-rotor mini-rotorcraft," in *Quad Rotorcraft Control*, pp. 23–34, Springer, 2013.

[33] E. G. Hernández-Martínez, G. Fernandez-Anaya, E. D. Ferreira, J.-J. Flores-Godoy, and A. Lopez-Gonzalez, "Trajectory tracking of a quadcopter uav with optimal translational control," *IFAC-PapersOnLine*, vol. 48, no. 19, pp. 226–231, 2015.

[34] J. Aguerrebere, E. Hernandez-Martinez, S. Montufar-Chavez, X. Tortolero-Baena, M. Salgado-Aguirre, G. Fernandez-Anaya, E. Ferreira-Vazquez, and J.-J. Flores-Godoy, "Quadcopter uav control based on input-output linearization and pid," in *2021 IEEE International Midwest Symposium on Circuits and Systems (MWSCAS)*, pp. 1003–1006, IEEE, 2021.

[35] T. Moons, L. Van Gool, M. Vergauwen, *et al.*, "3d reconstruction from multiple images part 1: Principles," *Foundations and Trends® in Computer Graphics and Vision*, vol. 4, no. 4, pp. 287–404, 2010.

[36] P. Wang, Z. Wang, S. Xin, X. Gao, W. Wang, and C. Tu, "Restricted delaunay triangulation for explicit surface reconstruction," *ACM Transactions on Graphics (TOG)*, 2022.

[37] J. Cortes, S. Martinez, T. Karatas, and F. Bullo, "Coverage control for mobile sensing networks," *IEEE Transactions on robotics and Automation*, vol. 20, no. 2, pp. 243–255, 2004.